



HAL
open science

Molecular profiling of matrix coated and native tissue sections by UV and IR MALDI-O-TOF-MS.

Klaus Dreisewerd, R. Lemaire, G. Pohlentz, M. Salzet, M. Wisztorski, S. Berkenkamp, I. Fournier

► To cite this version:

Klaus Dreisewerd, R. Lemaire, G. Pohlentz, M. Salzet, M. Wisztorski, et al.. Molecular profiling of matrix coated and native tissue sections by UV and IR MALDI-O-TOF-MS.. *Analytical Chemistry*, 2007, 79 (6), pp.2463 -2471. 10.1021/ac061768q . hal-00086947

HAL Id: hal-00086947

<https://hal.science/hal-00086947>

Submitted on 18 Aug 2007

HAL is a multi-disciplinary open access archive for the deposit and dissemination of scientific research documents, whether they are published or not. The documents may come from teaching and research institutions in France or abroad, or from public or private research centers.

L'archive ouverte pluridisciplinaire **HAL**, est destinée au dépôt et à la diffusion de documents scientifiques de niveau recherche, publiés ou non, émanant des établissements d'enseignement et de recherche français ou étrangers, des laboratoires publics ou privés.

**Molecular Profiling of Native and Matrix-Coated Tissue Slices from Rat Brain
by Infrared and Ultraviolet Laser Desorption/Ionization Orthogonal-Time-of-
Flight Mass Spectrometry**

Klaus Dreisewerd,[†] Remi Lemaire,[‡] Gottfried Pohlentz,[†] Michel Salzet,[‡] Maxcence Wisztorski,[‡]
Stefan Berkenkamp,[¶] Isabelle Fournier.[‡]

[†]*Institute of Medical Physics and Biophysics, Westfälische Wilhelms-Universität Münster, Germany*

[¶]*Sequenom GmbH, Hamburg, Germany*

[‡]*Laboratoire de Neuroimmunologie des Annélides, Université des Sciences et Technologies de Lille,
France*

Keywords:

Running Title: IR-LDI- and UV-/IR-MALDI-o-TOF-MS profiling of rat brain tissue

Address reprint requests to: Dr. Klaus Dreisewerd, Institute of Medical Physics and Biophysics,

University of Münster, Robert-Koch-Str. 31, D-48149 Münster; email: dreisew@uni-muenster.de

Abstract: Phospho- and glycolipids contained in the plasma membrane of neuronal tissue were profiled by direct infrared laser desorption/ionization orthogonal time-of-flight mass spectrometry (IR-LDI-o-TOF-MS), performed on cryosected native slices generated from rat brain. Spraying of potassium acetate onto the slices was found to facilitate data interpretation in positive ion mode by reducing residual sodium adduct ion intensities. The high mass resolving power of the instrument of $\sim 10,000$ (FWHM) along with an accuracy of the analysis in the low 10 ppm range allows a putative identification of the lipids and differentiation of variations in the fatty acid residues based on their molecular weight. Moreover standard histology glass slides can be used as substrates without degrading the mass accuracy of the analysis. Resolving power and mass accuracy are also independent of the laser wavelength and thickness of the tissue slices. Coating the slices with matrix and using an ultraviolet laser for UV-MALDI-o-TOF-MS extends the analysis to peptides and small proteins. Peptides and partially-cleaved proteins derived from proteolytic digests were recorded after incubation of native sections with trypsin and subsequent coating of the slices with MALDI matrix.

INTRODUCTION

Molecular profiling and spatially-resolved molecular imaging of biological tissue by matrix-assisted laser desorption ionization mass spectrometry (MALDI-MS) has recently found a wide research interest,^{1,2} for example to identify biological markers or for differential analysis studies.³ In its simplest form MALDI-MS profiling can allow a rapid analysis: simple mixing of a tissue (micro-) section with a suitable matrix can generate a profile of the major peptide/protein content, for example of neuroendocrine tissue,⁴ or that of the major phospho- and glycolipid constituents of the cell membranes.⁵ More sophisticated matrix preparation protocols allow to preserve the spatial distribution of analyte molecules within the tissue to a certain extent and to generate a molecular image by scanning the laser across the slices.⁶ Under ideal preparation conditions, the achievable lateral resolution would be as small as the focal laser beam diameter.⁷ However, owing to molecular diffusion, the spatial resolution is frequently diminished during the matrix application step. Direct laser desorption ionization (LDI) mass analysis of native slices avoids the critical preparation step. However, lacking the MALDI matrix, in conjunction with the direct analysis of biological tissue this approach has in the past essentially been limited to the analysis of small cations or anions within tissue slices and cells.^{8,9} Mostly ultraviolet (UV) lasers were used in these studies. Direct infrared (IR-)LDI analysis of peptides and small proteins from lyophilized samples¹⁰ or from protein-loaded polyacrylamide gels¹¹ has been reported in a few studies. In particular the use of the water of hydration as the “IR matrix” may have its merits for the analysis of tissue cryosections.¹⁰ However, for the analysis of peptides and proteins this latter approach seems to be restricted to samples containing exceedingly high concentrations of analyte.^{10,11} In contrast to UV-MALDI-MS, where only monolayers of material are desorbed at the ion detection threshold,¹² material on the order of 5-10 μm in thickness is typically ablated by a single IR laser pulse.¹³

In by far the most applications, “axial” time-of-flight (a-TOF) analyzers have hitherto been employed for direct MALDI tissue analysis.¹⁴ These instruments, in which the normal of the sample plate is collinear with the ion axis of the first field-free drift tube, have the advantage of a high ion transmission and a theoretically unlimited mass range but require well-defined electrical field conditions in the ion source (i.e., flat and preferably electrically well conducting surfaces). Moreover, they need to be operated under high-vacuum in the MALDI ion source. Owing to field distortion and charging effects, the preparation of tissue slices on non-conducting glass slides –as standard in histology– typically leads to a substantial loss in sensitivity and in the mass accuracy of the axial-TOF-MS analysis. Furthermore, any variation in the thickness of the samples requires adjustment of the instrumental calibration. Metallization of the glass substrate or sputtering of a metal layer onto the preparation can improve the performance (M. Wisztorski, unpublished data),¹⁵ but these protocols add additional costs and/or cumbersome preparation steps. Also unwanted side effects caused by the metallization (e.g., adduct formation between metal and analyte) may be a concern.

The use of orthogonal (o-)TOF-MS instrumentation,¹⁶ in which the initially wide kinetic energy distributions, imparted onto the ions during the laser desorption process, are first thermalized by multiple collisions with a background gas and ions are then extracted perpendicular to their original direction of motion, has recently been shown to permit a high constant mass accuracy of the analysis that is widely independent of the type and morphology of the sample surface.¹⁷ Moreover, laser fluence is a much less critical parameter than in axial-TOF-measurements. However, two disadvantages associated with the o-TOF-instrumentation are a potentially high abundance of background signals from matrix clusters as well as analyte-matrix adduct ion formation. Both effects can be attributed to the elevated background pressure in the ion source allowing for extensive ion-molecule reactions.¹⁸ Although the “continuous” ion extraction/time-to-digital conversion detection scheme makes the o-TOF-instrumentation ideally suited for operation with high-repetition rate lasers, substantial ion transfer times from the ion

source to the analyzer regions do limit high-throughput analysis. Owing to the high amount of material ablated per IR laser pulse, the decoupling of desorption/ionization and mass analysis is particularly beneficial for IR-MALDI-MS analysis and efficiently increases the accuracy of the analysis by about an order of magnitude if compared to IR-MALDI-MS-axial-TOF-MS. This way the high mass accuracy analysis of glycolipids directly from thin-layer plates is for instance straightforwardly possible.¹⁷ In a study performed in parallel to ours, Woods et al. recently reported the detection of some major phospholipids from matrix-coated and native brain tissue.¹⁹ Mostly sphingomyelin and phosphatidylcholine species were detected in this work realizing a coupling of direct IR-LDI with an hybrid ion mobility orthogonal extraction TOF mass spectrometer.

In the present paper, molecular profiling of cryosected native and matrix-coated rat brain tissue slices by IR-LDI-o-TOF-MS and by UV-/IR-MALDI-o-TOF-MS is reported. Phospho- and glycolipidspecies are tentatively assigned based on the mass of well resolved monoisotopic ions. Peptides and small proteins were detected by UV-MALDI-MS after coating of the slices with MALDI matrix. Tryptic digest products were detected after treating native slices with enzyme followed by matrix-coating.

EXPERIMENTAL

Abbreviations.

Diacylglycerol (DAG); fatty acid (FA); galactose (Gal); ceramide (Cer); N-acetyl neuraminic acid (NeuAc) Gal β 1-3GalNAc β 1-4(NeuAc α 2-3); Gal β 1-4Glc β -Cer (GM1); cerebroside (CB), α -cyano-hydroxycinnamic acid (HCCA); phosphatidic acid (PA); phosphatidylcholine (PC); phosphatidylamine (PE); phosphatidylglycerol (PG); phosphatidylinositol (PI); phosphatidylserine (PS); plasmeneylethanolamine (PlsEtn); sphingomyelin (SM); sulfatide (ST); hydroxylated sulfatide (ST-OH).

Materials. α -cyano-4-hydroxycinnamic acid (HCCA), sinapic acid, bradykinin fragment 1-7, substance P, melittin, and potassium acetate were obtained from Sigma-Aldrich (Deisenhoven, Germany) and used without further purification. Trypsin was from Promega (Framingham, MA).

Tissue preparation. Adult male Wistar rats weighing 250 - 350 g (animal use accreditation by the French ministry of the agriculture N° 04860) were maintained under standard care. Animals were sacrificed by decapitation and immediately dissected to remove the brain. Frozen sections Remi: from the xy part of the brain (= intereural 12.70 Bregma 3.70 to intereural 1.20 Bregma -7.80) of either 15 or 60 μ m were obtained with a cryotome and thaw-mounted onto standard histology glass slides.

Tryptic digest. 30 μ L of enzyme solution (33 ng/ μ L in 25 mM Tris buffer, pH 7.4) were applied onto tissue slices using a micropipette. To reduce solvent evaporation, samples were covered with a small dish. After digestion for either 3 or 10 minutes at room temperature, the slices were rinsed with 80% ethanol and allowed to dry at room temperature.

Sample preparation for LDI- and MALDI-MS analysis.

HCCA matrix solution was prepared by dissolving 10 - 20 mg of HCCA in 1 mL of acetonitrile/0.1%TFA (2:1, v/v). Sinapic acid matrix was prepared by dissolving 20 mg of sinapic acid in 1 mL of acetonitrile/0.1%TFA (1:1, v/v). A volume of matrix solution of 10 - 20 μ l was spread over the tissue sections using a micropipette. The sample was allowed to dry at room temperature, forming a homogeneous microcrystalline preparation. Cryosected tissue slices were stored at -20 or -70°C prior to use. For analysis, samples were thawed under air and condensed water was allowed to evaporate at room temperature. For LDI, samples were either transferred directly into the mass spectrometer or tissue slices were rewetted with 0.5 M of potassium acetate

using a pneumatic nebulizer. Transfer into the mass spectrometer was done after evaporation of solvent.

Orthogonal-TOF-Mass Spectrometer

The o-TOF-MS is a modified prototype, similar to the one described by Loboda et al.²⁰ By default, this instrument is equipped with an N₂ laser emitting 3 ns long pulses at a wavelength of 337 nm and a maximum repetition rate of 30 Hz. The UV laser beam is delivered via a fiber optical system, producing a spot size on the sample of $\sim 200 \times 230 \mu\text{m}^2$. In our modified version, a second laser port has been added to adopt the beam of an Er:YAG-laser (BiOptics Laser Systeme, Berlin, Germany). This laser emits pulses of ~ 100 ns in duration at a wavelength of 2.94 μm and a repetition rate of ~ 2 Hz. The IR laser beam irradiates the sample under an angle of incidence of 45°. The focal spot size is approximately $150 \times 200 \mu\text{m}^2$. Samples can be observed with a CCD camera and $\sim 10 \mu\text{m}$ resolution. To accommodate glass slides of up to $30 \times 50 \text{ mm}^2$ in size and 1.8 mm in thickness, the central part of the sample plate ($50 \times 30 \text{ mm}^2$) was milled out to a thickness of ~ 2 mm. An adapter was used for 1 mm thick microscopic slides. Substrates were fixed with double sided pads of 0.2 mm thickness.

Ions are generated in an elevated-pressure ion source filled with nitrogen gas ($p \sim 1 - 5 \times 10^{-1}$ mbar) and are accelerated by a low extraction field of ~ 25 V/mm into a quadrupole ion guide. The quadrupole is filled with N₂ at a pressure of $\sim 10^{-3}$ mbar. In normal operation the lower m/z cut-off of the quadrupole was set to m/z 500 in order to optimize ion transmission for the lipid and peptide mass range. To monitor low mass ions, this cut-off was set to m/z 150 in a few experiments. After passing the collisional cooling quadrupole, ions enter the high-vacuum part of the instrument ($p \sim 1 \times 10^{-7}$ mbar) where they are accelerated in orthogonal direction with respect to their original movement. Time-of-flight analysis was performed in both negative (-) and positive (+) ion mode, using acceleration potentials of 10 (-/+) or 20 kV (+) and a repetition rate of the push-out pulser of a few kHz. Time-to-digital measurements were typically performed with a bin width of 256 ps.

Calibration of the instrument was achieved with a two-point calibration using either protonated or deprotonated molecular ions of bradykinin fragment 1-7 and either substance P or melittin desorbed from a regular analyte/matrix preparation. For acquisition of UV-MALDI mass spectra ~7000 single laser pulses were typically applied according to an acquisition time of ~4 min at 30 Hz laser repetition rate. Owing to the lower repetition rate of the IR-laser of only 2 Hz and the larger amounts of material ablated per pulse, a maximum of ~1200 IR-laser pulses was applied for IR-LDI- and IR-MALDI-MS. Laser fluences were adjusted to values moderately above the ion detection threshold for the individual matrix/wavelength combinations. For analysis with the IR laser, the sample plate was typically moved to a neighboring position after a few to ~ ten single exposures whereas for UV-MALDI a few ten to some hundred laser pulses were typically applied on a certain position before the position was changed. Mass spectra were processed using the MoverZ3 software (vs. 2001.02.13, Genomic Solutions, Ann Arbor, MI).

RESULTS AND DISCUSSION

Direct IR-LDI-MS

Direct IR-LDI-o-TOF mass spectra that were acquired from a cryosected slice of 60 μm thickness in negative and positive ion mode, respectively, are plotted in Figures 1 and 2. The native slice was sprayed with 0.5 M KAc prior to the MS analysis. The mass spectra were recorded from random positions in a central area of the slice of approximately 5 x 5 mm^2 in size. In both ion modes, the mass spectra are dominated by a series of ions in the m/z -range between ~ 700 – 900 (Figures 1a, 2a). The mass ranges and characteristic mass differences of 2, 16, and 28, observed for several sets of ions (see for example insets in Figure 1a) suggest that these species represent phospholipids with varying fatty acid residues on the one hand, and glycolipids, in particular hydroxylated and non-hydroxylated sulfatides, on the other. Owing to the high mass resolution of ~ 10,000 (FWHM) of the analysis, the identity of these ions may tentatively be assigned based solely on their

monoisotopic mass. Major phospho- and glycolipid structures from rat brain tissue have been identified previously in several studies, for example by nano-ESI-tandem MS analysis.²¹ Likely identities of the detected species are proposed in Tables 1 and 2 for the two ion modes, respectively, along with theoretical m/z values and experimentally determined ones using external calibration. The generally good agreement between the values suggests that the detected ion species are indeed likely to represent several of the well-known major phospho- and glycosphingolipids of rat brain plasma membranes: hydroxylated and non-hydroxylated sulfatides (ST, ST-OH), cerebroside (CB), phosphatidylcholine (PC), phosphatidylethanolamine (PE), phosphatidylglycerol (PG), phosphatidylinositol (PI), plasménylethanolamine (PlsEtn), phosphatidylserine (PS), sphingomyelin (SM). Although variations in the fatty acid chain residues (i.e., the number of C-atoms and the degree of saturation), are straightforwardly detectable, the MS¹ data do not allow further differentiation as to the site of the modification. For example, the ion at m/z 885.54 (Figure 1b) could in principle represent an PI 18:1/16:0 or an PI 18:0/16:1, though the second isoform is naturally occurring in much higher abundance. A differentiation would be possible by tandem MS analysis, for example by using collisional activation. This option was not available on the employed prototype instrument. Tandem MS analysis would also allow for a safer identification of the head groups and thus type of the lipids. Partly, the distributions of likely lipids overlap too closely to allow a differentiation by the mere MS¹ data. For example, the ion at m/z 844.51, observed in positive ion mode (Table 2), could equally well represent a ST 38:2 (theoretical m/z , 844.50) or a PC 38:6 (844.53) species. Also PA and CB ion species are likely masked by overlapping lipid series.

The low mass ranges from m/z 130 - 600, recorded in negative and positive ion mode, respectively, are shown in Figures 1b and 2b. The likely identity of some of these low-intensity ions are indicated in the figures. Generally, direct IR-LDI induces only very little fragmentation of the lipids. Only for the most abundant PC's some sizable intensity of PC-N(CH₃)₃ ion species is observed in positive

ion mode (Table 2), next to some lyso-PC's ions of minor abundance (Table 2, Figure 2b). In negative ion mode, mainly alkylates (16:0, m/z 255.24; 18:0, m/z 283.27; 18:1, m/z 281.26) could be assigned. Further exploration of the identity of low mass species was beyond the scope of the present work.

In the negative ion mode, two species that are presumably representing singly sialylated gangliosides, namely GM1 36:1 (theoretical m/z of the deprotonated molecule, 1544.87) and GM1 38:1 (theoretical m/z , 1572.90), are furthermore detected (Figure 1c). Overlap with unspecific dimeric ions of smaller phospho- and glycolipids, that are produced within the laser desorption ionization process, renders the identification of possible further ganglioside species difficult. In positive ion mode, distinct ganglioside species could not be differentiated from the background of "unspecific" gas phase dimers of smaller lipids (Figure 2c), e.g., (PC 34:1)₂K⁺ at m/z 1558.10 (theoretical m/z , 1558.09).

Expectedly, more acidic phospholipids are preferentially (or exclusively) detected in the negative ion mode, whereas neutral phospholipids are eventually only detected through cationization with sodium or potassium (e.g., PC). Some species (e.g., SM, PE) are detected with comparable intensity in both ion modes. Presumably owing to the high natural concentration of potassium in rat brain, even for desorption from native slices positively charged lipids are almost exclusively represented potassiumated molecules [M+K]⁺. Only the most abundant phospholipids also generate [M+Na]⁺ ions of some intensity (Table 2). Spraying of the native slices with KAc further reduced their intensity and, hence, facilitates data interpretation. Rupture of the cell membranes is not expected to occur as a consequence of the application of KAc solution. A slight drawback is the fact that potassium exhibits a distribution of naturally occurring isotopes which contains about 7% of ⁴¹K, overlapping with lipids being also two Dalton apart because of a different degree of saturation in their fatty acid residues. Peptide ions of notable intensity do not seem to be produced

by direct IR-LDI. Unspecific fragment ions stemming from these and other cell constituents are, however, likely to contribute to the chemical background.

Table 1 and 2 also provides some information about the relative fatty acid variations within lipid species of a particular type. The degree of saturation or varying chain lengths are not expected to influence the ion yield sizably, nor to influence a potential fragmentation substantially. A comparison of lipid species of different type would be substantially less straightforward due to the rather different ionization efficiencies. For a more valid quantitave analysis, $^{12}\text{C}/^{13}\text{C}$, $^{39}\text{K}/^{41}\text{K}$ isotopic abundances, as well as potential overlap with the distributions of other species need to be further taken into account. Within these limitations, the determined ion abundances suggest, for example, that the ratio of singly unsaturated PC (34:1) to fully saturated PC (34:0) is approximately 2:1 - 3:1 (Table 2), whereas the PC 36:1 to PC 36:0 yield would be somewhat higher and about 3:1 - 4:1. Concerning the repartition of lipids and unsaturated species : PC:32:0 has a strong signal in cerebellar cortex (rim of the brain) and is low in cerebellar peduncle (Woods et al, Anal Chem, 2005, 77, 4523-4527). Cerebellar peduncle is in the middle down of the brain (see added data). Klaus, we maybe see a difference between this part and the rest of the brain ...

IR-MALDI-MS

Abundant lipid ions are also produced by IR-MALDI-MS from HCCA-coated slices (Figure 3a,b). Owing to the higher intensities of sodiated, and the additional generation of protonated ion species, mass spectra recorded in the positive ion mode are more complex than for IR-LDI-MS. Overall, the same lipid species as by IR-LDI are, however, recorded in positive ion mode. In the negative ion mode, some phospholipids (notably PE, PlsEtn, SM), that are detected in medium to high abundance by IR-LDI (Figure 1b), are apparently suppressed in the IR-MALDI mass spectra (Figure 3a). A similar effect is observed in UV-MALDI-MS (data not shown). This observation comes as a surprise because only part of the tissue (by size below 50%) is visibly covered with

HCCA matrix. The suppression may be attributed to extensive gas phase reactions taking place in the expanding MALDI plume and thermodynamically favoring certain products. Alternatively, also the use of a relatively nonpolar solvent, containing 50% acetonitrile, may lead to the observed loss. Further studies are needed to evaluate these effects in more detail. Different matrix systems like 2,5-dihydroxybenzoic acid, which is more commonly used for the analysis of lipids, may also facilitate their detection by MALDI-MS. IR-MALDI-o-TOF-MS analysis of neither HCCA- or sinapic acid coated slices hardly produced any (peptide) ions with molecular weights in excess of 1000 (data not shown). Only some very abundant peptides (as determined by UV-MALDI-MS; see below) produce some ions also in IR-MALDI. This observation may be attributed to a general lower ionization efficiency for peptides of the IR-MALDI mode. Notably, the degree of matrix cluster formation was found to rather low if not absent for both IR-MALDI ion polarities.

UV-MALDI-MS

UV-MALDI-o-TOF-MS analysis of HCCA-coated slices extends the detectable mass range to about 10,000 Da. Figure 4a displays an UV-MALDI-o-TOF mass spectrum that was recorded from an HCCA-coated slice in positive ion mode. The use of sinapic acid extended the accessible mass range even further – to about an m/z of 40,000 (data not shown). The negative ion mode produced only comparatively low ion abundances for both matrices (data not shown). Ions above 1000 Da are in their majority believed to represent peptides and small proteins.² As demonstrated by the insets in Figures 4a, up to about an m/z of ~9000 ¹²C-isotopic resolution is achieved by the o-TOF-analysis. In comparison to typical axial-UV-MALDI-TOF measurements from tissue slices,²² this constitutes a substantial improvement. An experiment, in which neighboring slices have been analyzed in parallel by axial- and o-TOF-MS, showed that essentially the same peptides are, however, detected by both methods (data not shown). Further going peptide identification was beyond the scope of the present study

High abundances of phospholipid and sulfatide ions are also generated by positive ion mode UV-MALDI (Figure 4b), by pattern essentially identical to those recorded in the IR-MALDI-MS analysis (Figure 3a). Alike for peptides, lipid ion abundances are substantially lower in negative ion mode mass spectra (data not shown). The potential overlap with smaller peptides (e.g., the ion observed at m/z 943.47 in Figure 4b probably presents such a peptide) and matrix cluster ions complicate the data interpretation. A few matrix cluster ions are assigned in Figure 4b with an asterisk - these species were identified from a mass spectrum that was taken from a pure matrix sample. The degree of matrix cluster formation is notably higher for UV- than for IR-MALDI. Adduct complexes between analyte (both lipid and peptide) and matrix can form another concern, in particularly if cinnamic acid derivatives are employed as matrix.^{23,24} The extent of adduct formation seems to depend critically on the exact sample preparation conditions - such complexes were in fact observed in a minority of the performed experiments. Comparing standard microcrystalline peptide/matrix MALDI preparations and the preparations on lipid rich tissue, the degree of both matrix cluster and adduct complex formation was generally found to be much lower for the tissue preparations – or even essentially absent, like in the mass spectrum displayed in Figure 4.

A substantial drawback accompanying MALDI imaging of tissue is the easy delocalization of molecules from their original lateral position during the matrix preparation step. Indeed, medium intensities of lipids and peptides were well detected from an area just next to the slices to which matrix (and analytes) have eluted during the matrix preparation step (data not shown). Although this problem is clearly aggravated if –like in the current work– rather simple sample preparation protocols are employed, it clearly poses one of the major obstacles for laterally well-resolved MALDI-MS imaging. In contrast, any major delocalization by polar solvents (including the almost unavoidable condensed water) is rather unlikely to play a significant role on the ten-micrometer

scale. Recondensation of laser ablated material onto the slices was not observable visually, though molecular redosition may be a general concern in spatially resolved analysis. For example, IR irradiation of a position just next to the tissue slice, that was previously extensively wetted with aqueous KAc solution, did not produce any lipid ion signals.

UV-MALDI-MS analysis of tissue treated with trypsin

Molecular identification based on the mass of the detected ion alone is hardly ever unequivocal. Immunology may provide specific identification but is restricted to individual target structures (Salzet, M.; Wattez, C.; Slomianny, M.C.; *Comp. Biochem. Physiol. Comp. Physiol*, 1993, 104, 75-81).^{ref salzet?} MALDI tandem-MS may be used for structural analysis and identification of small molecules directly from tissue sections but would typically be limited to ions not exceeding 2000 – 3000 Da in mass. Enzymatic digestion of peptidergic components contained – and being accessible to the enzyme – in the tissue may form an interesting “shotgun” approach to cleave larger peptides and proteins to product ion sizes falling well into this mass range (reference for this strategy : digestion of proteins coated on PVDF membrane : Chaurand, P.; Stoeckli, M.; Caprioli, R.M.; *Anal.Chem*, 1999, 71, 5263-5270). Large proteins that are not detectable by direct MALDI-MS of the original tissue sample may even become demasked. Owing to the high number of enzymatic fragment ions, that will in general be produced by this approach, a high resolving power of the mass spectrometer for differentiation of precursor ion species will be compulsory.

Figure 5 demonstrates the principle feasibility of this approach. In this experiment, trypsin was applied for 3 min before the slice was rinsed with ethanol and HCCA matrix was added. Besides for the tryptic peptides this approach also produces a set of larger (and new) ions with m/z values up to above ~25,000. These species presumably represent partially cleaved larger proteins that do not show up in the mass spectrum taken from the untreated sample. Autolysis ions of trypsin could not

be identified. The exceedingly large number of ion signals in the tryptic fragment mass range renders a data bank search less meaningful but the results clearly demonstrate that tandem-MS analysis on such a preparation should be possible. Applying trypsin for longer times leads to more complete digestion but also more complex mass spectra (data not shown), and may help to produce fragment ion sizes amenable for tandem MS analysis.

CONCLUSIONS

Molecular analysis of tissue slices employing a MALDI ion source operated at an elevated pressure of ~1 mbar and combined with an orthogonal TOF mass analyzer provides several advantageous features. The analysis can be performed with slices of almost arbitrary thickness without degradation of a high and mass-independent resolving power of about 10,000. For convenience and compatibility with histology, tissue slices can also be prepared on standard glass substrates. The employment of an IR-laser allows to generate spatially-resolved phospho- and glycolipid profiles even from native cryosected slices. Spraying of a concentrated KAc solution onto the slices was found to facilitate data interpretation in positive ion mode by effectively reducing the formation of sodium-adduct ions. An important feature of the direct LDI approach is that analyte diffusion is essentially avoided and data recorded as a function of lateral position thus reflect a “true” image of the lipid distribution, at least on a micrometer scale. We will address this issue of achievable lateral resolution further in succeeding work employing smaller laser sizes. In contrast to UV- or IR-MALDI-MS, matrix-less IR-LDI produces no protonated lipids, suggesting additional ionization pathways being effective in the MALDI-case. UV-MALDI-o-TOF-MS allows the precise profiling of peptides and small proteins from matrix-coated tissue with equally high mass resolution. Larger proteins can partially be demasked by treatment of the tissue with trypsin. Employing miniaturized digestion and matrix preparation protocols in combination with structural analysis and protein

identification by tandem MS may therefore allow spatially resolved shot-gun proteomics directly from tissue slices.

ACKNOWLEDGEMENT

The authors are grateful to Sequenom GmbH (Hamburg, Germany) for use of their o-TOF-instrument. We would also like to thank Franz Hillenkamp for support of the project, and Andreas Rohlfing and Sarah Kruppe for technical assistance. Supported by grants from Centre National de la Recherche Scientifique (CNRS), Ministère de la Recherche et des Technologies (MRT, ACI jeunes Chercheurs to I. Fournier), Fondation pour la Recherche Médicale (FRM, to I. Fournier), Génopole-Lille to M. Salzet. Financial support by the Deutsche Forschungsgemeinschaft (grant DR 416/5-1) is furthermore acknowledged.

Table 1. Putative identities of phospho- and glycolipid species observed by direct IR-LDI-o-TOF-MS from native rat brain tissue slice in the negative ion mode, along with the theoretical and experimental m/z -values of the monoisotopic deprotonated molecular ion, $[M-H]^-$.^{a,b}

^a slices were sprayed with 0.5 M KAc prior to the analysis

^b to guide the eye, lipids detected with high signal intensity (> 1000 a.u.) are highlighted

abbreviations: galactose (Gal); ceramide (Cer); N-acetyl neuraminic acid (NeuAc) Gal β 1-

3GalNAc β 1-4(NeuAc α 2-3); Gal β 1-4Glc β -Cer (GM1); phosphatidic acid (PA phosphatidylamine

(PE); phosphatidylglycerol (PG); phosphatidylinositol (PI); phosphatidylserine (PS);

plasmenylethanolamine (PlsEtn); sphingomyelin (SM); sulfatide (ST); hydroxylated sulfatide (ST-

OH).

Experimental m/z	Theoretical m/z	Identity	Signal Intensity arb. units.	Alternatives
599.33	599.32	Lyso-PI 18:0		
670.52	670.46	PA 34:2	507	
673.51	673.52	SM 32:1	222	or PA 34:1 (673.48)
699.49	699.50	PA 36:2	904	
700.51	700.53	PlsEtn 34:1	1019	
701.51	701.55	SM 34:1	1019	
702.51	702.54	PlsEtn 34:2	448	
715.57		PA 36:2 + OH ?	907	
716.56	716.52	PE 34:1	626	
718.55	718.54	PE 34:0	409	
726.53	726.54	PlsEtn 36:2	1021	
728.56	728.56	PlsEtn 36:1	1288	
742.56	742.54	PE 36:2	487	
744.55	744.55	PE 36:1	742	
745.53	745.50	PG 34:2		
746.54	746.51	PlsEtn 38:7	689	
747.53	747.52	PG 34:1	843	
748.52	748.53	PlsEtn 38:5	825	
750.53	750.54	PlsEtn 38:4	934	
752.57	752.56	PlsEtn 38:3		
754.56	756.58	PlsEtn 38:2	404	
756.59	756.59	PlsEtn 38:1	315	
762.49	762.53	PS 34:0	530	+ PE 16:0/22:6 =762,5 (PE 38 :6) ? (ESI Q TOF identification)
764.51	764.52	PE 38:5	389	

766.54	766.54	PE 38:4	1096	
770.56	770.57	PE 38:2	221	
772.56	772.59	PE 38:1	646	
773.54	773.53	PG 36:2		
774.55	774.54	PlsEtn 40:7	983	
775.55	775.55	PG 36:1		
776.56	776.56	PlsEtn 40:6	743	
778.57	778.58	PlsEtn 40:5	754	
788.51	788.54	PS 36:1	566	
790.53	790.56	PS 36:0	1114	+ PE 40:6 ?
792.54	792.55	PE 40:5	660	
794.56	794.57	PE 40:4	765	
806.53	806.54	ST 36:1	1114	
821.54		PI 32:2 + OH ?	765	
822.55	822.54	ST-OH 36:1	720	
834.56	834.58	ST 38:1	1142	
835.56	835.53	PI 34:1	1036	
849.54		PI 34:2 + OH		
850.55	850.57	ST-OH 38:1	354	
857.51	857.52	PI 36:4	1178	
860.58	860.59	ST 40:2	530	
862.61	862.61	ST 40:1	1048	
876.60	876.59	ST-OH 40:2	803	
878.61	878.60	ST-OH 40:1	1807	
883.52	883.53	PI 38:5	1508	
885.54	885.55	PI 38:4	13256	
887.56	887.56	PI 38:3		
888.61	888.62	ST 42:2	9915	
890.63	890.64	ST 42:1	7943	
902.62	902.60	ST-OH 42:3	614	
904.62	904.62	ST-OH 42:2	6092	
906.62	906.63	ST-OH 42:1	5574	
908.64	908.65	ST-OH 42:0	3173	ST-OH 42:0
916.67	916.66	ST 44:2	599	
918.65	918.67	ST 44:1	604	
920.64		ST 44:0 ?	343	
932.64	932.65	ST-OH 44:1	528	
934.65	934.64	ST-OH 44:0	361	
1544.88	1544.87	GM1 36:1	1124	
1572.91	1572.90	GM1 38:1	736	

Table 2. Putative identities of phospho- and glycolipid species observed by direct IR-LDI-o-TOF-MS from native rat brain tissue slice in the positive ion mode, along with the theoretical and experimental m/z -values of the monoisotopic cationized ions, $[M+K]^+$ and $[M+Na]^+$.^{a,b,c}

^a slices were sprayed with 0.5 M KAc prior to the analysis

^b the type of cation is denoted in brackets; protonated lipid species are not detected by IR-LDI, though they are generated by UV- and IR-MALDI.

^c to guide the eye, lipids detected with high signal intensity (> 1000 a.u.) are highlighted

abbreviations: Diacylglycerol (DAG); phosphatidylcholine (PC); phosphatidylamine (PE);

phosphatidylserine (PS); plasmenylethanolamine (PlsEtn); sphingomyelin (SM); sulfatide (ST);

hydroxylated sulfatide (ST-OH).

Experimental m/z	Theoretical m/z	Identity	Signal Intensity	alternatives
478.32	478.33	Lyso-PC 16:0	129	
504.32	504.35	Lyso-PC 18:0		
551.50	551.50	DAG ⁺ 32:0		
577.50	577.52	DAG ⁺ 34:1	127	
694.50		Pls 32:2 (Na ⁺)?	129	
697.45	697.47	PC-N(CH ₃) ₃ 32:0 (Na)	127	
710.47	710.45	PlsEtn 32:2 (K)	879	PlsEtn 32:2 (Na) + OH
712.47	712.46	PlsEtn 32:0 (K)	203	PlsEtn32:3(Na)+OH
713.44	713.45	PC-N(CH ₃) ₃ 32:0 (K)	771	
715.44		SM 32:0(K)?	336	
723.48	723.53	PC-N(CH ₃) ₃ 34:1 (Na)	160	SM34:2(Na)
725.48	725.55	PC-N(CH ₃) ₃ 34:0 (Na)	128	
727.48		SM32:0(K)+OH?	72	
737.44	737.45	PC-N(CH ₃) ₃ 34:2 (K)	130	
738.53	738.53	CB 34:1 (K)		PlsEtn34:2(K)
739.45	739.47	PC-N(CH₃)₃ 34:1 (K)	3155	SM34:2(K)
740.45		PlsEtn34:1(K)?		
741.46	741.48	PC-N(CH₃)₃ 34:0 (K)	1093	
743.48		SM34:0 (K)?		
748.58		PlsEtn36:4(Na)?	198	
751.40		SM36:2(Na)?	175	
753.59	753.59	SM 36:1 (Na)	266	
756.53	756.55	PC 32:0 (Na)	462	
758.54		?		
761.44	761.47	PG 32:0 (K)	568	
763.44	763.47	PC-N(CH ₃) ₃ 36:3 (K)	198	
765.47	765.48	PC-N(CH ₃) ₃ 36:2 (K)	279	
767.48	767.50	PC-N(CH₃)₃ 36:1 (K)	1276	SM36:2(K)

768.49	768.53	PlsEtn 36:1 (K)		
769.53	769.56	SM 36:1 (K)	2145	PC-N(CH₃)₃ 36:0 (K) (769.51)
770.54	770.55	PlsEtn 36:0 (K)		
771.55		SM 36:0 (K) ?	713	
772.55	772.53	PC 32:0 (K) probably 16:0/16:0 (ESI Q TOF)	3818	
782.54	782.57	PC 34:1 (Na)	928	
784.55	784.58	PC 34:0 (Na)	846	
789.47	789.50	PG 34:0 (K)	571	
793.50	793.51	PC-N(CH ₃) ₃ 38:2 (K)		
795.55	795.58	SM 38:2 (K)		PC-N(CH ₃) ₃ 38:1 (K) (793.53)
796.51	796.53	PC 34:2 (K)	551	
798.53	798.54	PC 34:1 (K) probably 16:0 / 18:1 (ESI Q TOF)	14166	
800.53	800.56	PC 34:0 (K)	5018	
804.45		?PC 38: 8 (H+) ?	401	
806.47		?PC 38:6 (H+) ?	48	
810.57	810.60	PC 36:1 (Na)	504	
812.57	812.61	PC 36:0 (Na)	359	PC 34:2+OH (K) .?
820.54	820.53	PC 36:4 (K)	2302	
822.51	822.54	PC 36:3 (K)	1107	
824.55	824.56	PC 36:2 (K)	382	
826.55	826.57	PC 36:1 (K)	5671	
828.59	828.59	PC 36:0 (K)	1391	
834.50		PC 36:2+OH(K)?	164	
840.43	840.47	ST 36:4 (K)	291	
842.45	842.48	ST 36:3 (K)	214	
844.51	844.50	ST 36:2 (K)	1819	PC 38:6 (K) (844.53)
846.52	846.52	ST 36:1 (K)	1004	PC 38:5 (K) (846.54)
848.53	848.56	PC 38:4 (K)	2190	
851.61	851.64	SM 42:2 (K)		
852.45		PC38:2(K)?	652	
853.61	853.66	SM 42:1 (K)	?	
854.62	854.60	PC 38:1 (K)	409	
855.62		SM 42:0?	?	
856.48	856.47	ST-OH 36:4 (K)	225	PC 40:6 + Na + ?
858.52	858.48	ST-OH 36:3 (K)	109	
863.36		?	192	
866.68		ST38:5(K)?	196	
868.45	868.50	ST 38:4 (K)	1014	
870.46		ST38:3(K)	427	
872.54	872.53	ST 38:2 (K)	1168	PC 40:6 (K) (872.56) Probably 18:0/22:6 (ESI Q TOF)
874.55	874.55	ST 38:1 (K)	409	PC 40:5 (K) (874.57)
876.57	876.59	PC 40:4 (K)	274	
878.59	878.60	PC 40:3 (K)	112	
880.46		PC 40:2 ?	85	
882.64	882.64	PC 40:1 (K)	114	
908.64		PC 42:2 (K) ?		
910.66		PC 42:1 (K)?		
934.42		?		
936.42		?		

950.39		?		
952.40		?		
963.47		?		
965.48		?		

FIGURE CAPTIONS

Figure 1. Direct IR-LDI-o-TOF mass spectra recorded from a 60 μm -thick rat brain tissue slice in negative ion mode. The tissue slice was sprayed with 0.5 M KAc solution prior to the analysis. (a) m/z -range from 600 - 1050, displaying a series of phospholipid and hydroxylated and non-hydroxylated sulfatide species. Major ions are assigned with their putative identity (see Table 1 for an extensive list). All ions represent deprotonated molecular species, $[\text{M}-\text{H}]^-$. The inset shows an enlarged section showing the m/z range from m/z 850 - 900. (b) M/z range from 130 – 600; this spectrum was recorded with the low m/z cut-off of the quadrupole set to 150. (c) M/z range from 1350 – 1700 displaying two putative GM1 ganglioside ions; all other ions presumably represent “unspecific“ phospholipid dimers that are produced during the desorption ionization process.

Figure 2. Direct IR-LDI-o-TOF mass spectra recorded from a 60 μm -thick rat brain tissue slice in positive ion mode. The tissue slice was sprayed with 0.5 M KAc solution prior to the analysis. (a) m/z -range from 600 - 1050, displaying a series of phospholipid and sulfatide species. Major ions, are assigned with their putative identity (see Table 2 for an extensive list). All major ions represent $[\text{M}+\text{K}]^+$ ions. (b) M/z range from 130 – 600; this spectrum was recorded with the low m/z cut-off of the quadrupole set to 150. (c) M/z range from 1350 – 1700. Presumably only unspecific phospholipid dimers, produced during the desorption ionization process are detected.

Figure 3. IR-MALDI-o-TOF mass spectrum recorded from a 60 μm -thick HCCA-coated rat brain tissue slice in (a) negative and (b) positive ion mode, displaying a series of phospho- and glycolipid species. Some major ions are assigned with their putative identity. In negative ion mode, all ions represent deprotonated molecular species, $[\text{M}-\text{H}]^-$. In positive ion mode, $[\text{M}+\text{H}]^+$, $[\text{M}+\text{Na}]^+$, and $[\text{M}+\text{K}]^+$ ions are observed with comparable intensities.

Figure 4. UV-MALDI-o-TOF mass spectra recorded from a 60 μm -thick HCCA-coated rat brain tissue slice in positive ion mode. (a) full mass spectrum (m/z 500 – 14,250). The insets demonstrate the high mass resolution throughout the recorded mass range. M/z values are given for the ^{12}C -monoisotopic peak except for high mass ions for which average molecular weights, denoted by brackets $\langle \rangle$, are indicated. (b) M/z -range from 600 to 1050, displaying a series of phospho and glycolipid ions. Some major ions are assigned with their putative identity. Ions are observed with comparable intensities as $[\text{M}+\text{H}]^+$, $[\text{M}+\text{Na}]^+$, or $[\text{M}+\text{K}]^+$ ions as demonstrated by the inset. Identified matrix cluster ion signals are labeled with an asterisk. “/ *” denotes that matrix cluster and lipid ions could not be distinguished. The acceleration potential of the TOF analyzer was set to 20 kV to favor the detection of larger ions.

Figure 5. UV-MALDI-o-TOF mass spectra recorded in positive ion mode from a 15 μm -thick rat brain tissue slice, after allowing enzymatic digestion with trypsin directly on the slice for 3 min (at room temperature). The digestion reaction was stopped by rinsing the slices with 80% ethanol and subsequent application of HCCA matrix.

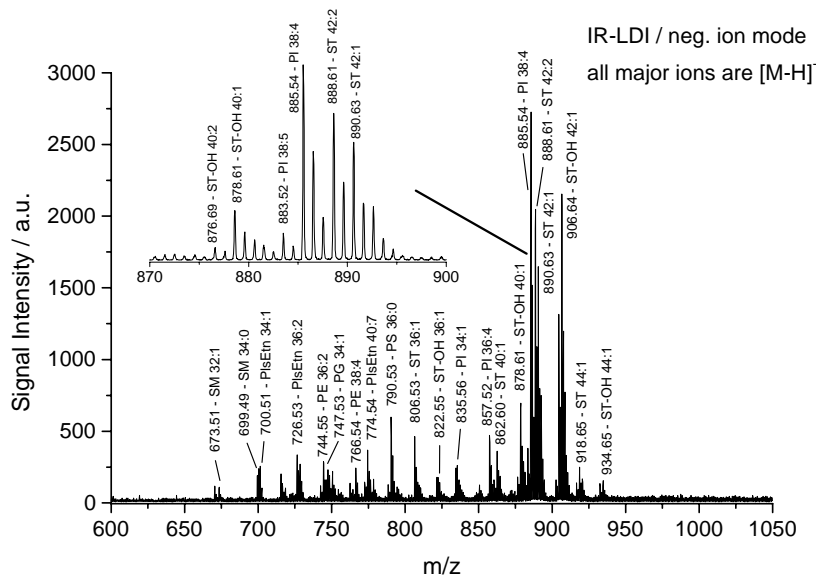


Figure 1a

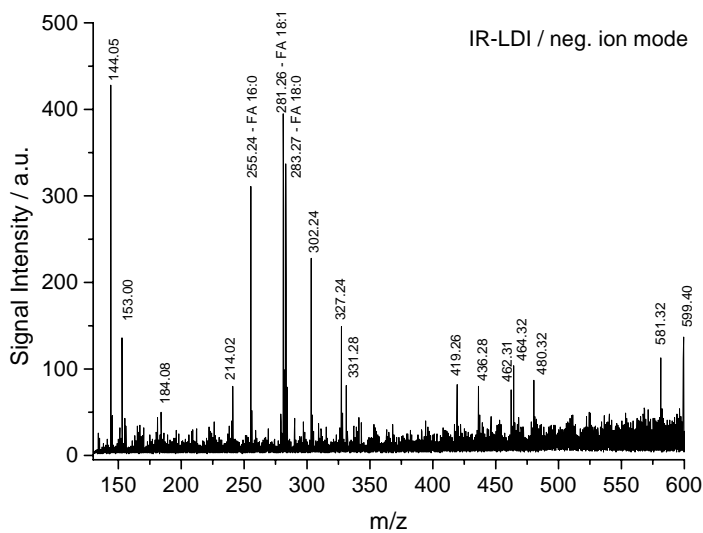


Figure 1b

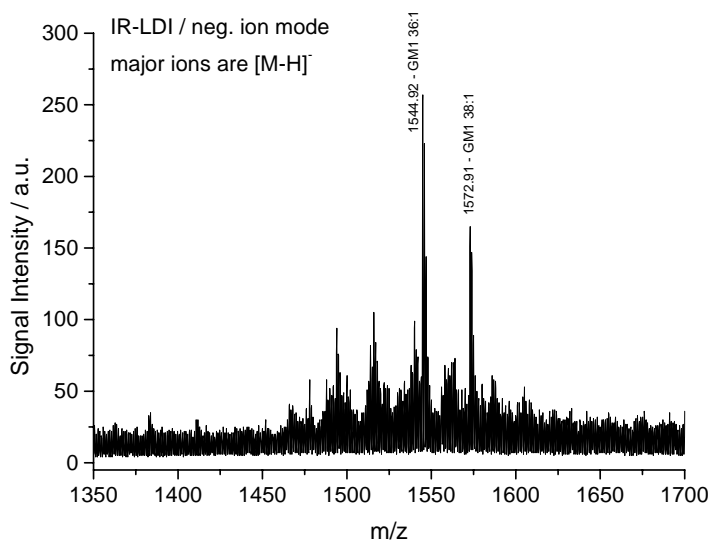


Figure 1c

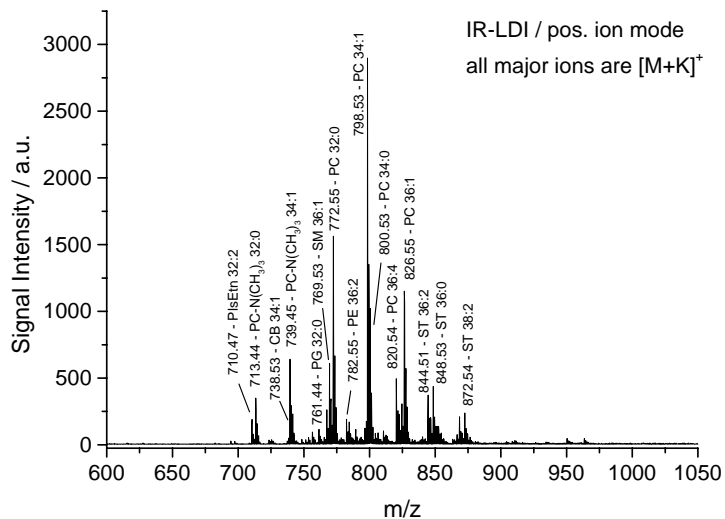


Figure 2a

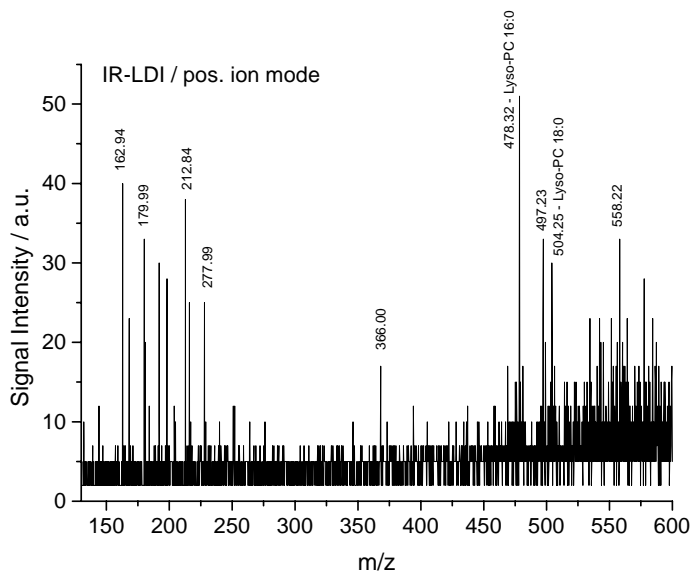


Figure 2b

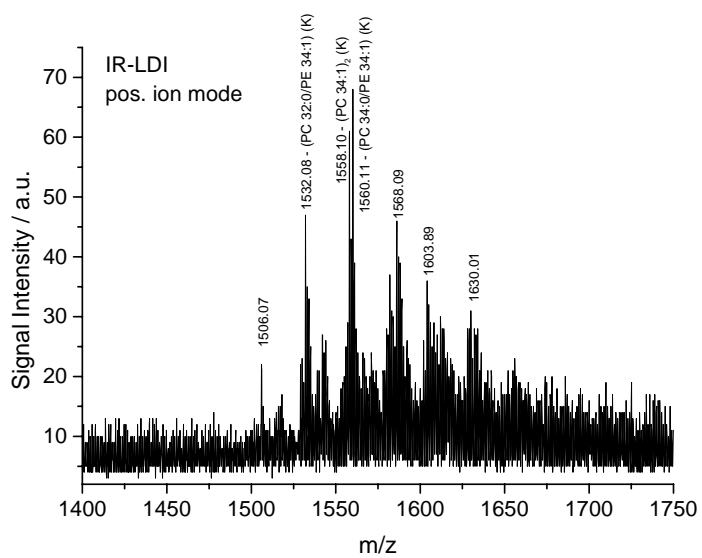


Figure 2c

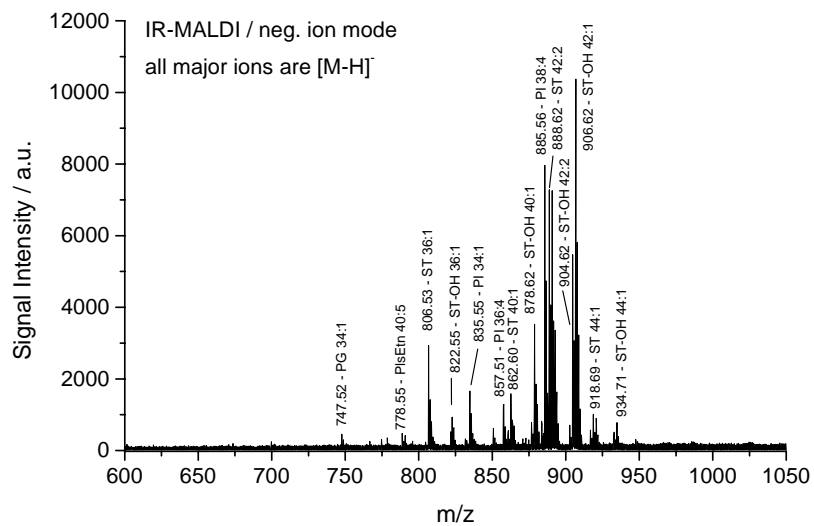


Figure 3a

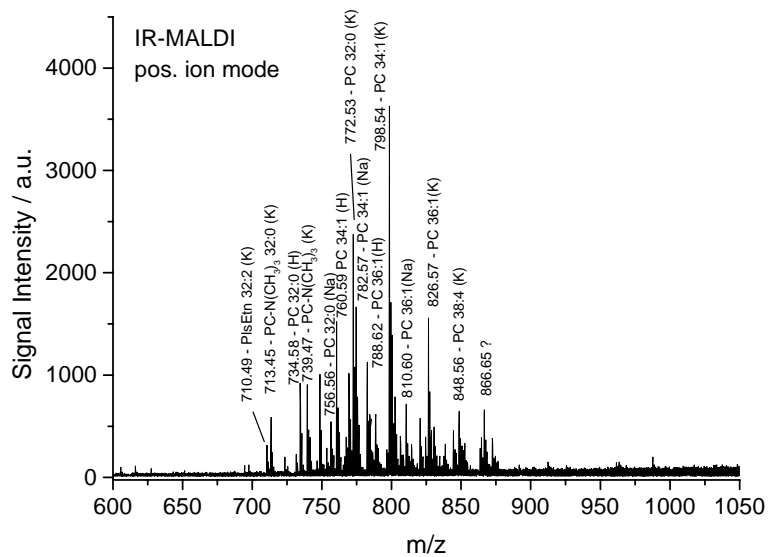


Figure 3b

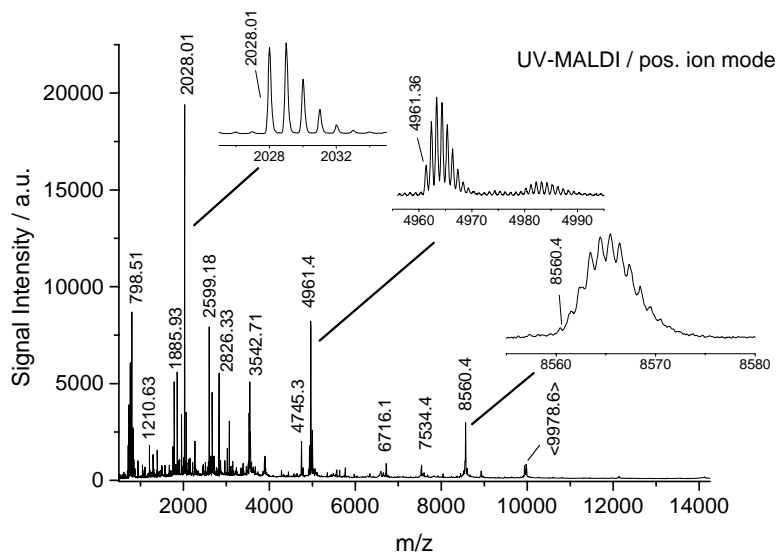


Figure 4a

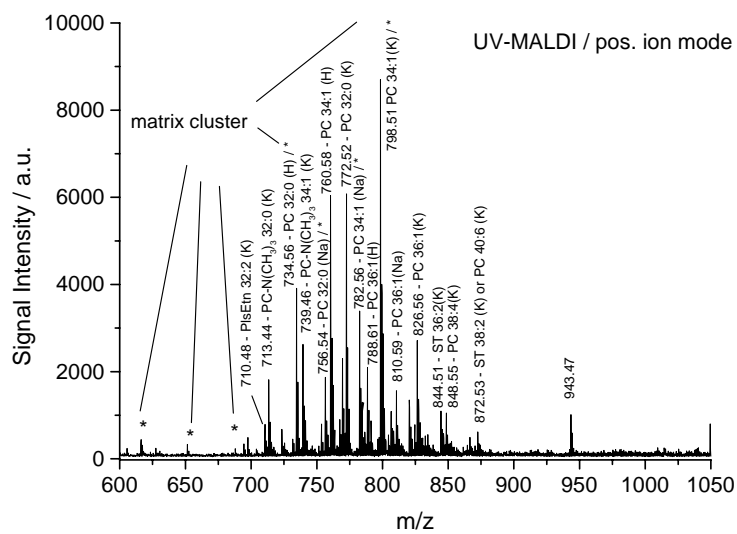


Figure 4b

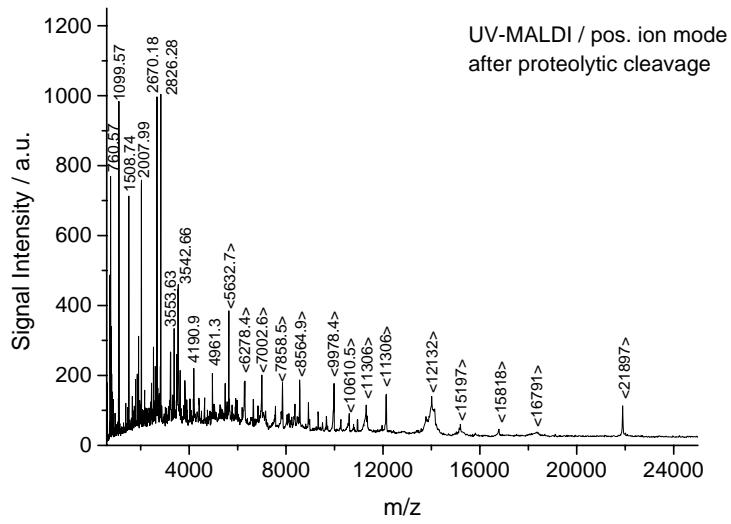


Figure 5

REFERENCES

- 1 Caldwell, R. L.; Caprioli, R. M., *Mol. Cell. Proteom.* **2005**, *4*, 394.
- 2 Chaurand, P.; Schwartz, S. A.; Caprioli, R. M. *Anal. Chem.* **2004**, *76*, 87A-93A.
- 3 Fournier, I.; Day, R.; Salzet, M. *Neuroendocr. Lett.* **2003**, *24*, 9
- 4 Dreisewerd K.; Kingston, R.; Geraerts, W. P. M.; Li, K. W. *Int. J. Mass Spectrom.* **1997**, *169*, 291.
- 5 Jackson, S. N.; Wang, H. Y. J.; Woods, A. S. *Anal. Chem.* **2005** *77* 4523.
- 6 Schwartz, S.; Reyzer, M. L.; Caprioli, R. M. *J. Mass Spectrom.* **2003**, *38*, 699.
- 7 Spengler, B.; Hubert, M. *J. Am. Soc. Mass Spectrom.* *2002*, *13*, 735.
- 8 Proceedings of LAMMA Symposium, Düsseldorf, Germany, October 8-10, 1980, *Fres. Z. Anal. Chem.*, **1981**, Vol. 308.
- 9 Hillenkamp, F.; Unsold, E.; Kaufmann, R.; Nitsche, R., *Appl. Phys.* **1975**, *8*, 341.
- 10 Berkenkamp, S.; Karas, M.; Hillenkamp, F. *Proc. Nat. Acad. Sci. USA* **1996**, *93*, 7003.
- 11 Rousell, D. J.; Dutta, S. M.; Little, M. W.; Murray, K. K. *J. Mass Spectrom.* **2004**, *39*, 1182.
- 12 Dreisewerd, K. *Chem. Rev.* **2003**, *103*, 395.
- 13 Menzel, C.; Dreisewerd, K.; Berkenkamp, S.; Hillenkamp, F. *Int. J. Mass Spectrom.* *2001*, *207*, 73-96.
- 14 Chaurand, P.; Reyzer, M. L., Caprioli, R. M. in M. Gross, R. M. Caprioli (Eds.) *Encyclopedia of Mass Spectrometry*, Elsevier, 2004, Vol. 2, pp. 339.
- 15 Delcorte, A.; Bour, J.; Aubriet, F.; Muller, J. F.; Bertrand, P. *Anal. Chem.* *2003*, *75*, 6875.
- 16 Krutchinsky, A. N.; Loboda, A. V.; Spicer, V. L.; Dworschak, R.; Ens, W.; Standing, K. G. *Rapid Commun. Mass Spectrom.* **1998**, *12*, 508.
- 17 Dreisewerd, K.; Muthing, J.; Rohlfing A.; Meisen I.; Vukelic, Z.; Peter-Katalinic, J.; Hillenkamp, F.; Berkenkamp, S. *Anal. Chem.* **2005**, *77*, 4098.
- 18 Loboda, A. V.; Chernushevich, I. V. *Int. J. Mass Spectrom.* **2005**, *240* 101.

- 19 Woods, A. S.; Ugarov, M.; Jackson, S. N.; Egan, T.; Wang, H. Y. J.; Murray, K. K.; Schultz, J. *A. J. Proteome Res.* **2006**, *5*, 1484.
- 20 Loboda, A. V.; Ackloo, S.; Chernushevich, I. V. *Rapid Commun. Mass Spectrom* **2003**, *17*, 2508.
- 21 Lemaire, R. ; Wisztorski, M.; Desmons, A.; Tabet, J.C. ; Day, R. ; Salzet, M. ; Fournier, I. *Anal. Chem.*, **in press**.
- 22 Lemaire, R.; Tabet, J. C.; Ducoroy, P.; Hendra, J. B.; Salzet, M.; Fournier, I. *Anal. Chem.*, **2006**, *78*, 809.
- 23 Ivleva, V. B.; Elkin, Y. N.; Budnik, B. A.; Moyer, S. C.; O'Connor, P. B.; Costello, C. E. *Anal. Chem.* **2004**, *76*, 6484.
- 24 Krutchinsky, A. N.; Chait, B. T. *J. Am. Soc. Mass Spectrom.* **2002**, *13* 129.